

An Active Handheld Device for Compensation of Physiological Tremor using an Ionic Polymer Metallic Composite Actuator*

Abhijit Saxena, *Student Member, IEEE* and Rajni V. Patel, *Fellow, IEEE*

Abstract— Involuntary motions of the hand can have a significant deteriorating effect on the performance of microsurgical procedures such as vitreoretinal microsurgery. The most common source of the involuntary motions is physiological tremor. Real-time compensation of physiological tremor is therefore necessary to assist surgeons to accurately perform a microsurgery. A novel approach based on the use of Ionic Polymer Metallic Composites (IPMCs) has been developed for actively compensating physiological tremor in the hand. We present the design of our novel handheld device that compensates for tremor using an IPMC-based actuator. We then experimentally evaluate the device to show the amount of compensation achieved.

I. INTRODUCTION

Physiological tremor is inherent in all humans. It is an involuntary motion that is approximately rhythmic and roughly sinusoidal [1]. It puts a limitation on the accuracy of tasks that require precise manipulation such as microsurgery, military targeting or hand-held photography. During certain procedures such as ophthalmological, neurological or inner ear microsurgeries, it is difficult to precisely position a tool-tip due to physiological tremor [2]. One such procedure is vitreoretinal surgery in which a surgeon is required to remove tissues as thin as 20 μm from the retina. The rms amplitude of a tool-tip due to tremor during vitreoretinal surgery has been reported to be 24 μm , 22 μm and 20 μm along the x, y and z axes respectively [3]. It has also been reported that the frequency of physiological tremor in the wrist ranges from 8 to 12 Hz [4]. The accuracy of such procedures depends on the experience of the surgeons and the dexterity of surgeons' hands.

One of the methods to compensate for physiological tremor in the hand during microsurgical procedures is an active handheld device. An active handheld device senses its own motion, filters tremulous from non-tremulous motion and compensates for tremor by deflection of its tool-tip. It is an attractive solution for tremor compensation because of its cost-effectiveness as well as familiarity for surgeons (similar to a conventional passive handheld device). However, the challenge in developing such a device is that it must be

lightweight (<50 g) and compact in size so as to reduce the fatigue resulting from holding it for long periods of time.

An alternative to handheld devices is a technology that uses a robotic system, e.g., the Steady-Hand Robot (SHR) [5]. In the SHR, the robotic arm provides tremor-free positional control of the surgical tool that is held both by the user and the robotic arm. Another early technology includes a master-slave telerobotic system, the Robot Assisted Microsurgery system (RAMS) [6]. Robotic systems are bulkier and costlier compared to handheld devices; therefore, these methods were not considered in our work.

One of the most significant contributions towards an active handheld microsurgical device is the Micron [7][8]. An early prototype of Micron, as reported in [7], used inertial sensors for motion sensing and piezoelectric actuators for deflection of the tool-tip and weighed 100 g. Further developments on Micron were reported in [8] in which the authors used an optical tracking system for direct position measurement of the tool-tip. The prototype, as reported in [8], uses piezoelectric 'bending' actuators and weighs 40g. Another handheld device, the SMART [9], uses optical coherence tomography to sense the hand tremor. It employs a piezoelectric motor for compensation of tremor and weighs 65 g. These prototypes have shown the feasibility of using an active handheld device for tremor compensation. In order to further reduce the weight and size, and thus increase the user acceptance of the handheld devices, we have investigated the use of ionic polymer metallic composites (IPMCs) [10] for tremor compensation. These materials, as described in Section II, are small and lightweight, and therefore have the potential for use in a compact configuration suitable for a handheld device.

In this paper, we present a novel active handheld device which we have called an Accuracy Improvement Device (AID). The AID senses its own motion using small inertial sensors, estimates the motion incurred due to tremor using a filtering algorithm followed by deflection of its tool-tip using a small IPMC actuator. Our approach resulted in a device that weighs 23.56 g and allows changing the size of the device in order to enhance the user experience.

The rest of the paper is organized as follows. Section II presents the system design that includes the design specification of the handheld device, a filtering algorithm for estimating the position of the needle-tip subject to tremor, an open-loop controller for the IPMC actuator and an overview of the integrated system. Section III presents an experimental setup to assess the performance of the system followed by a discussion of the results. Finally, Section IV provides concluding remarks.

*This research was supported by the Natural Sciences and Engineering Research Council (NSERC) of Canada through grants RGPIN1345 (Discovery) and 371322-2009 (CREATE Program), and by infrastructure grants from the Canada Foundation for Innovation and the Ontario Research Fund awarded to the London Health Sciences Centre (Canadian Surgical Technologies & Advanced Robotics - CSTAR) and to the University of Western Ontario (UWO).

A. Saxena and R.V. Patel are with CSTAR, London, ON N6A 5A5, Canada and the Dept. of Electrical and Computer Engineering, UWO, London, ON N6A 5A5, Canada. R.V. Patel is also with the Dept. of Surgery, UWO. (e-mail: abhijit.saxena@lhsc.on.ca, rvpatel@uwo.ca).

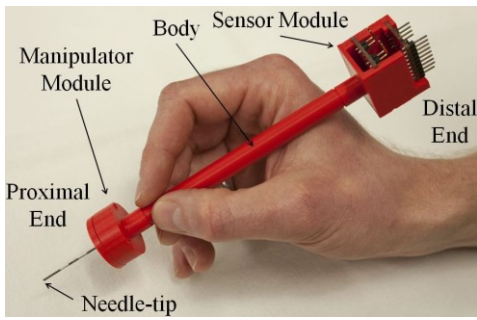


Figure 1. Prototype of the handheld device, AID, built at CSTAR.

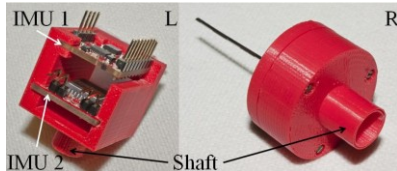


Figure 2. Left: Sensor module of the AID; Right: Manipulator module of the AID.

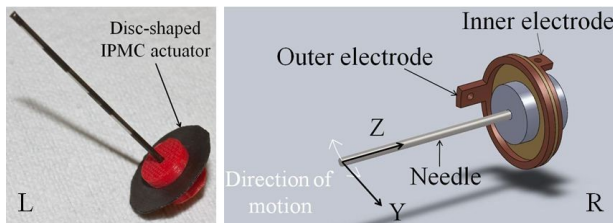


Figure 3. Internal components of the manipulator module. Left: IPMC actuator with attached needle; Right: CAD rendering of the internal components of the manipulator module and the direction of motion of the needle. The IPMC actuator is shown in gold. The two (outer and inner) ring-shaped copper electrodes are shown in dark brown. The components shown in grey are used to fix the needle to the IPMC actuator.

II. SYSTEM DESIGN

A. Instrument Design

Fig. 1 shows a prototype of the device. It is 192 mm long (including a 35 mm needle at the proximal end) and is composed of three parts: a sensor module at the distal end, a manipulator module at the proximal end and a body that attaches the sensor and the manipulator modules.

The sensor module, shown in Fig. 2, measures the motion of the hand in six degrees of freedom (DOF) using two inertial measurement units (IMUs). The IMU, marked as IMU 1 in Fig. 2, contains a tri-axial accelerometer (ADXL 335- Analog Devices) and a dual-axis gyroscope (IDG 500- InvenSense). The IMU, marked as IMU 2 in Fig. 2, contains a single-axis gyroscope (MLX 90609- Melexis). Both the IMU boards contain signal-conditioning circuits that limit the bandwidth of the sensors to 50 Hz.

The body of the AID where the user holds the device has an outer diameter of 10 mm. It is a hollow shaft so that the wires from the manipulator module can reach the distal end of the device. Both the sensor and the manipulator modules contain a hollow shaft, as shown in Fig. 2, using which they are attached to the body to completely assemble the device.

We have chosen an ionic polymer metallic composite (IPMC) for actuation of the needle-tip. An IPMC is composed of a thin strip of ionomer (Nafion or Flemion) plated with a noble metal such as gold or platinum on both sides [10]. When an electric field is applied across the metal plates, the IPMC shows deformation towards the anode. In comparison to electroactive ceramics (EACs), IPMCs are lighter and require low voltages (< 5 V). IPMCs also show a higher range of strains as compared to EACs. The strain using EACs can be increased using mechanical amplification; however, it increases the size and the weight of the system. In contrast to shape memory alloys (SMAs), IPMCs have significantly faster response time than SMAs. IPMCs can also be fabricated in any shape and size.

We have designed a disc-shaped IPMC actuator having an inner diameter of 5 mm, an outer diameter of 15 mm and a thickness of 1 mm. Fabrication of the IPMC actuator based on our design specifications was performed by Environmental Robots Inc. The needle is attached to the IPMC actuator using the inner circumference of the disc as shown in Fig. 3. The IPMC actuator, with the needle attached to it, is held between two ring-shaped copper electrodes using the outer circumference of the disc as shown in Fig. 3. When a sinusoidal voltage input of 3.5 V and frequency 15 Hz is applied across the copper electrodes, the actuator tilts the needle, as shown in Fig. 3, and positions it along the Y axis with peak-to-peak (p-p) amplitude of approximately 1 mm; this motion generates a negligible amount of motion along the Z axis. The manipulator module containing the disc-shaped IPMC actuator is shown in Fig. 2.

The use of IPMC as an actuator allowed the device to be light in weight and compact in size; the total weight of the prototype shown in Fig. 1 is 23.56 g. The outer diameter and the thickness of the manipulator module (without the needle and shaft) are 27 mm and 13.3 mm respectively. The other advantages of the design is that the length of the device and the diameter of the gripping area can be modified based on the user's need to enhance the ergonomics of holding the device. This can be done by changing the dimensions of the body since it does not contain any sensors or actuators.

B. Algorithm to calculate tremor

Fig. 4 shows the kinematic representation of the device. We attach a body frame $\{B\}$ at the center of the tri-axial accelerometer such that the sensing axes of the accelerometer are coincident with the principal axes of $\{B\}$. Two frames, $\{G1\}$ and $\{G2\}$ are attached at the center of the dual-axis gyroscope and single-axis gyroscope respectively. A frame $\{S\}$ is attached at the non-tremulous position of the needle-tip. The orientation of $\{S\}$ is the same as that of $\{B\}$.

One of the ways to calculate the real-time tremor motion of the needle tip is to calculate the position of the needle tip with respect to the world coordinate system $\{W\}$ followed by filtering out the non-tremulous motion using a zero-phase adaptive band-pass filter [11]. However, this method requires the knowledge of 3-DOF orientation. It has been well documented in the literature [11] [12] that the estimation of 3-DOF orientation requires the use of a complementary sensor such as a tri-axis magnetometer along

with a tri-axis accelerometer and a triad of gyroscopes or with three dual-axis accelerometers. The 3-DOF orientation can then be calculated by using data fusion techniques such as a Kalman filter. The use of an additional sensor increases the size and the weight of the system.

We have developed an algorithm to calculate the 3-DOF tremor motion of the needle-tip that requires the knowledge of only 2-DOF orientation. Since the 2-DOF orientation can be calculated using a combination of a tri-axis accelerometer and a triad of gyroscopes and a Kalman filter, the algorithm resulted in further reduction in the size and weight of the device because an additional sensor is not required. The algorithm is similar in approach to the one reported in [13] with the following modifications: (1) instead of using three dual-axis accelerometers to sense the motion, we have used the sensor module presented in the previous section; (2) we have removed the gravity force from the accelerometer measurements using 2-DOF orientation; and (3) we have designed a Kalman filter to estimate the 2-DOF orientation. Fig. 5 shows a block diagram of our algorithm. The goal of the algorithm is to calculate the position of the needle-tip due to tremor with respect to the frame $\{S\}$ from the sensor measurements provided by the sensor module.

The signal measured by the tri-axis accelerometer (y_a) is modeled as,

$$y_a = {}^B A + {}^B G \quad (1)$$

where ${}^B A = [{}^B a_x \quad {}^B a_y \quad {}^B a_z]^T$ is the linear acceleration vector and ${}^B G$ is the gravity force vector. The signal measured by the gyroscopes (y_g) is modeled as,

$$y_g = {}^B \omega + b \quad (2)$$

where ${}^B \omega = [{}^B \omega_x \quad {}^B \omega_y \quad {}^B \omega_z]^T$ is the angular velocity vector and $b = [b_x \quad b_y \quad b_z]^T$ is the gyro bias vector.

Using (1), the effective acceleration with respect to $\{B\}$ can be written as,

$${}^B A = y_a - {}^B G \quad (3)$$

$${}^B A = y_a - ({}^W R_B)^{-1} {}^W G \quad (4)$$

where ${}^W R_B$ is the rotation matrix that describes the orientation of the frame $\{B\}$ with respect to the frame $\{W\}$. ${}^W G = g[0 \quad 0 \quad 1]^T$ is the gravity vector with respect to the frame $\{W\}$ and g is the gravity constant. The Z-Y-X Euler angle notation is used to describe the rotation matrix since the sensors rotate with the device. Therefore, (4) becomes,

$${}^B A = y_a - g[-s\theta \quad c\theta s\varphi \quad c\theta c\varphi]^T \quad (5)$$

where φ and θ represent the Euler angles which are defined as angular rotations about X_B and Y_B respectively. It is clear from (5) that only 2-DOF orientation (φ and θ) is required to calculate the effective linear acceleration.

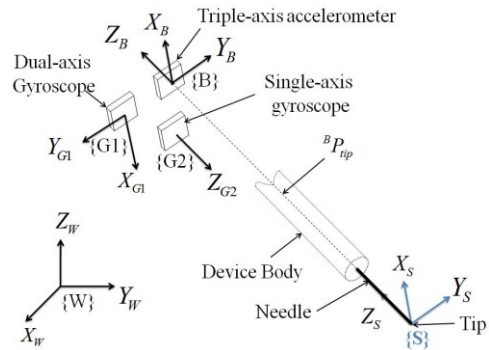


Figure 4. Kinematic representation of the device with respect to a world coordinate frame $\{W\}$.

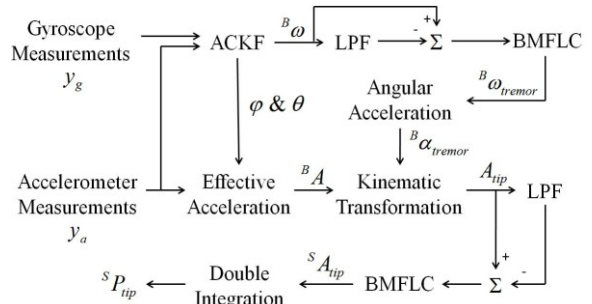


Figure 5. Block diagram of the algorithm to estimate the position of the needle-tip due to tremor. ACKF is an augmented state complementary Kalman filter. LPF is a fourth-order low-pass filter with a cut-off frequency of 4 Hz. The pass-band frequency of BMFLC is 7-13 Hz.

We have designed an augmented-state complementary Kalman filter (ACKF) that fuses the accelerometer and gyroscopic measurements (y_a and y_g respectively) to provide a drift-free and reduced noise estimation of the Euler angles, φ and θ . The ACKF also provides the unbiased angular velocity vector (${}^B \omega$) that is composed of the angular velocity due to tremor motion, non-tremulous motion, gyro noise and residual gyro bias. It is sent to a fourth order low-pass filter (LPF) with a cut-off frequency of 4 Hz. The output of the LPF is subtracted from its original input (${}^B \omega$) as shown in Fig. 5. This step removes the angular velocity due to non-tremulous motions such as voluntary motion and the residual gyro bias and provides the angular velocity due to tremor motion, residual low-frequency components and gyro noise. It has been shown in [13] that this low-pass filtering technique does not change the phase of the signal. The output of the subtraction is sent to a zero-phase adaptive band-pass filter, Bandlimited Multiple Fourier Linear Combiner (BMFLC) [14] that estimates the angular velocity due to tremor (${}^B \omega_{tremor}$) as shown in Fig. 5.

The acceleration at the needle-tip can be written as the sum of the linear acceleration at $\{B\}$, the centripetal acceleration and the tangential acceleration of the device,

$$A_{tip} = {}^B A + {}^B \omega \otimes ({}^B \omega \otimes {}^B P_{tip}) + {}^B \alpha \otimes {}^B P_{tip} \quad (6)$$

where \otimes is the cross product, ${}^B P_{tip} = [0 \quad 0 \quad 0.19]^T$ is the position of the needle tip with respect to the frame $\{B\}$ and ${}^B \alpha = [{}^B \alpha_x \quad {}^B \alpha_y \quad {}^B \alpha_z]^T$ is the angular acceleration

vector. For microsurgical procedures, the term $|\omega^2|$ is very small and can be ignored. Therefore, (6) becomes,

$$A_{tip} = {}^B A + {}^B \alpha \otimes {}^B P_{tip}. \quad (7)$$

The angular acceleration is calculated using the angular velocity due to tremor,

$${}^B \alpha_i = \frac{{}^B \omega_{tremor, i, k} - {}^B \omega_{tremor, i, k-1}}{T} \quad (8)$$

where $i = x, y$ and z and T is the sampling time. Using ${}^B \alpha_{tremor}$ and ${}^B A$, the acceleration at the needle-tip (A_{tip}) is calculated using (7). A_{tip} is composed of the acceleration due to tremor motion, non-tremulous motion, residual gravity and noise. The low-frequency components of A_{tip} are removed using the similar low-pass filtering technique as for the angular velocity as shown in Fig. 5. The acceleration of the needle-tip due to tremor (${}^S A_{tip}$) is estimated using the BMFLC. Since the tremor is essentially rhythmic in nature, the position of the needle-tip due to tremor (${}^S P_{tip}$) is calculated by double integration of ${}^S A_{tip}$ as presented in [14]. The results of estimating hand tremor using the proposed algorithm can be found in [15].

C. IPMC Controller

In the current implementation, to demonstrate feasibility of using IPMCs for tremor compensation, the prototype of the AID incorporates a 1-DOF IPMC-based manipulation system that compensates for the tremor in Y_S axis. With a known position of the needle-tip due to tremor (${}^S P_{tip}$), the goal of the manipulator module is to position the needle-tip in the negative of ${}^S P_{tip}$. Since compensation is shown in 1-DOF, the control-input (${}^C P$) becomes,

$${}^C P = -({}^S P_{tip, y}) \quad (9)$$

where ${}^S P_{tip, y}$ is the position of the needle-tip due to tremor in Y_S axis. In [16], the authors reported that the output displacement is approximately linear with respect to the voltage input applied to the IPMC if the input is sinusoidal. Since ${}^C P$ is sinusoidal, we have designed an open-loop gain-based controller for the IPMC actuator. Fig. 6 shows a block diagram of the controller. The controller model is defined as,

$${}^C V = K {}^C P \quad (10)$$

where ${}^C V$ is the amount of voltage required by the IPMC actuator to position the needle-tip at ${}^C P$ and K is the transformation factor. The value of K is 85715 that is obtained by empirically characterizing the IPMC actuator based on driving the actuator by various sinusoidal voltage inputs and measuring the displacements. Since the maximum voltage for IPMC actuator was specified as ± 3.75 V, the limiter block limits the voltage ${}^C V$ to ± 3.6 V. The voltage after the limiter block (${}^C \tilde{V}$) is sent to the manipulator module that positions the needle tip at ${}^C P$.

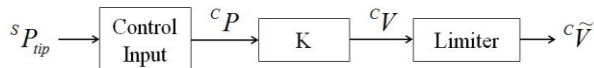


Figure 6. Block diagram of the gain-based open-loop IPMC controller.

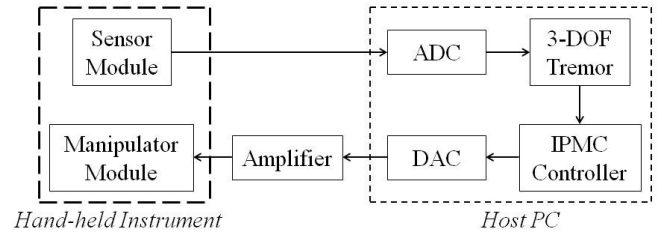


Figure 7. Overview of the system. The blocks inside the long-dashed lines are the part of the handheld device. The blocks inside the short-dashed lines are executed in the host PC.

D. Overview of the System

Fig. 7 shows an overview of the complete system. The blocks inside the short-dashed lines are executed in the host computer which is a Pentium 4, 2.8 GHz, 3GB RAM desktop computer with Windows XP Professional as the operating system. The analog-to-digital (ADC) and digital-to-analog (DAC) converter is a Sensoray 626 (Sensoray Co. Inc.) data acquisition board that is a PCI bus card with 16 16-bit differential analog input channels and 4 14-bit analog output channels. A real-time hardware-in-the-loop environment is created using QuaRC (Quanser) and the software for the system is programmed using Simulink and Matlab.

The 3-DOF accelerometer and gyroscopic measurements are sent to the host computer via the ADC. Using the sensor measurements, the 3-DOF position of the needle-tip due to tremor is estimated using the algorithm presented in the previous section. With the knowledge of ${}^S P_{tip}$, the amount of voltage (${}^C \tilde{V}$) necessary for compensation of tremor is calculated using the open-loop gain-based controller described in the previous section. The voltage is sent to an amplifier (UPM 2405- Quanser) via the DAC. The output of the amplifier is sent to the ring-shaped electrodes of the manipulator module to drive the IPMC actuator. The IPMC actuator compensates for the tremor by positioning the needle-tip in the opposite direction to that tremor.

III. EXPERIMENTAL EVALUATION

This section presents the experimental setup to evaluate the performance of the AID in achieving tremor compensation followed by an analysis of the results. In the experiments, we calculated the amount of compensation achieved with the AID by measuring the vibrations using a capacitive sensing method while the AID was given vibratory sinusoidal motion using a motorized linear stage.

A. Methodology

In the capacitive sensing method (CM), the capacitance (C) between two parallel plates of area (A) kept at a distance (d) apart is measured and is given by,

$$C = \frac{k\epsilon_0 A}{d} \quad (11)$$

where k is the relative permittivity of the dielectric material between the plates and ϵ_0 is the permittivity of the space. With known initial distance between the plates and

measuring the capacitance between the plates when one of the plates is fixed and the other is vibrating, the displacement between the plates due to the vibrations can be calculated using (11). In the experiments, a copper plate M was attached to the manipulator module of the device as shown in Fig. 8. The combined weight of the plate ‘M’ and the component holding the plate M was 5.5 gm which was significantly heavier than the combined weight (0.7 gm) of the needle and the component holding the needle. Since the AID tilts the tool-tip to provide compensation, the errors due to the tilting motion of the plate M on the capacitance were not accounted for in the experiments. More accurate experimental methods exist such as optical sensing that will eliminate the use of the plate and, thus, will not change the dynamics of the measurements; however, the goal of our experiments was to test the device using a quick and inexpensive method.

Fig. 9 shows the experimental set-up for measuring the amount of compensation by the AID using CM. The AID, with plate M, was attached on a precision motor linear stage (marked as ‘LS’, TLSM50A (Zaber Technologies) as shown in Fig. 9. A copper plate F, similar to the plate M, was kept fixed and parallel to the plate M to create a parallel-plate capacitor. The capacitance between the two plates was measured using PICOCAP evaluation kit (Acam). The area of both the plates M and F was 600 mm^2 . The tremor was simulated along the Y_s axis (shown in Fig. 9) using LS.

Since the physiological tremor is roughly sinusoidal and its frequency ranges from 8 to 12 Hz, LS was given sinusoidal input with frequencies ranging from 8 to 12 Hz. Two sets of experiments were conducted. In the first set, we tested the effect of frequency on the performance of the AID. We performed three experiments in which LS was given sinusoidal input with the following frequencies: 8, 10 and 12 Hz. The p-p amplitude of the input to LS was selected as $80 \text{ }\mu\text{m}$. This allowed us to test the effects of different frequencies on the performance of the AID. In the second set of experiments, we tested the effect of the amplitude on the performance of the AID by varying the amplitude of the input vibrations and keeping the frequency constant.

For each experiment, the plates (M and F) were initially kept at a known distance apart (d_o). The plate M was vibrated with the frequency for that experiment, as listed in Table I, using LS along the Y_s axis. The compensation by the AID was started after 10 seconds. The capacitance (C_{data}) between the plates M and F was measured and the data was stored in the computer.

The distance (D) between the plates M and F was calculated using,

$$D = \frac{k\epsilon_o A}{C_{data}} \quad (12)$$

where $A = 600 \text{ mm}^2$. The displacement of plate M with respect to plate F due to the vibrations measured using CM was calculated using,

$$D_{vibration} = D - d_o \quad (13)$$

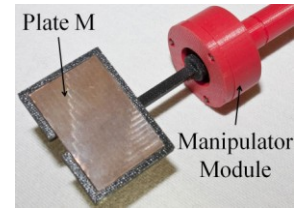


Figure 8. The plate M attached on the manipulator module of the AID.

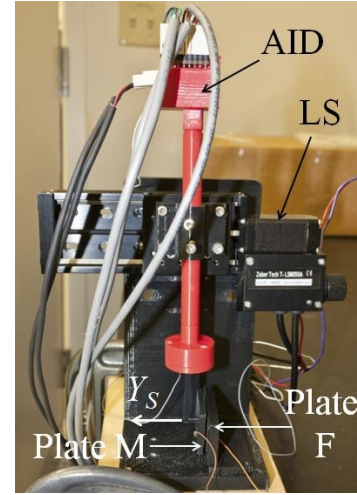


Figure 9. Experimental set-up for measuring amount of compensation using the AID. The figure shows the AID attached on a precision motor linear stage (LS) that simulates tremor in Y_s axis. The plate M, attached on the AID, and the plate F forms a parallel-plate capacitor.

B. Results and Discussion

Using $D_{vibration}$, we calculated the rms value of the displacement of the plate M with respect to the plate F before and after the compensation was started ($D_{UC, RMS}$ and $D_{C, RMS}$ respectively) followed by calculating the amount of compensation (AoC) achieved with the AID using,

$$AoC (\%) = \frac{D_{UC, RMS} - D_{C, RMS}}{D_{UC, RMS}} \times 100 \quad (14)$$

The displacement of plate M with respect to plate F due to the vibrations ($D_{vibration}$) measured using CM for a period of 5 seconds is shown in Fig. 10. The displacement before 10 seconds is the uncompensated vibration of plate M (i.e., D_{UC}) while the displacement after 10 seconds is the vibration of plate M after the compensation was started using the AID (i.e., compensated vibrations, D_C).

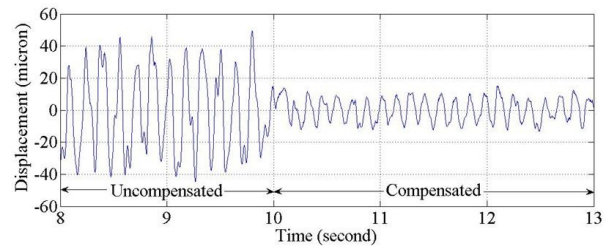


Figure 10. Displacement of the plate M with respect to the plate F due to the vibrations for a period of 5 seconds calculated using the capacitive sensing method for the first experiment.

TABLE I. EFFECT OF FREQUENCY ON THE AMOUNT OF COMPENSATION ACHIEVED WITH THE AID

f (Hz)	$D_{UC, RMS}$ (μm)	D_C, RMS (μm)	AoC (%)
8	25.45	7.39	70.96
10	26.40	9.65	63.44
12	26.84	10.50	60.87

The rms displacement of plate M before the compensation ($D_{UC, RMS}$) was 25.45 μm . The rms displacement of plate M after the compensation was started using the AID (D_C, RMS) was 7.39 μm which shows a reduction by 70.96%. Table I shows the amount of compensation achieved with the AID calculated using (14) for the frequencies selected in the experiments. Table I indicates that a higher amount of compensation was achieved for lower frequencies of the input vibrations. This is because the displacement of the IPMC actuator is higher at lower frequency and an open-loop gain-based controller has been used. These results demonstrate that the AID can compensate for vibrations in the frequency range of physiological tremor in the hand.

In addition to studying the effects of frequency, we also performed experiments to assess the effect of amplitude on the performance of the AID. The p-p amplitude of the input to the LS was decreased from 80 μm to 75 μm in the case of the 10 Hz frequency. The decrease in the amplitude resulted in an increase in the amount of compensation from 63.44% to 70.78%. Similarly, the peak-to-peak amplitude of the input to the LS was increased from 80 μm to 100 μm in the case of the 12 Hz frequency. The amount of compensation reduced from 60.87% to 56.19%. Therefore, the AID achieved a higher amount of compensation for lower amplitudes of vibration which suggests that the displacement of the IPMC actuator was the limiting factor in achieving a higher amount of compensation.

The copper plate (plate M) that was attached to the IPMC actuator during the experiments to measure the performance of the AID was significantly heavier than the needle and resulted in an increase in the load on the actuator during these experiments. A higher load decreases the displacement of the actuator, thereby reducing the amount of compensation achieved with the AID. In an actual handheld device, the IPMC actuator would drive a lighter needle, and therefore a higher amount of compensation would be achieved.

We establish that the amount of compensation achieved by the AID is dependent on the frequency and amplitude of the input vibrations. Our experiments clearly demonstrate that using an IPMC actuator, we can achieve a significant reduction in the amount of vibrations that could be typically incurred due to physiological tremor in the hand.

IV. CONCLUSION

In this paper, we presented the design and implementation of a novel approach for compensation of physiological tremor in a handheld microsurgical device. The prototype described in the paper demonstrated the feasibility of using Ionic Polymer Metallic Composites (IPMCs) for tremor

compensation. The use of IPMCs allows the device to be compact in size and light in weight. While tremor compensation in 1-DOF was shown experimentally, extension to multiple DOFs is possible without significant increase in complexity. In our ongoing work, a more sophisticated controller is being designed to enhance the motion compensation capability and increase the amount and robustness of the compensation in the all 3-DOFs.

REFERENCES

- [1] G. Grimaldi and M. Manto, *Tremor: From Pathogenesis to Treatment*, Synth. Lect. Biomed. Eng. 20, pp. 1-212, 2008.
- [2] M. Patkin, "Ergonomics Applied to The Practice of Microsurgery," *Aust. & N. Z. J. Surg.*, vol. 47, no. 3, pp. 320-329, June 1977.
- [3] S.P.N. Singh and C.N. Riviere, "Physiological Tremor Amplitude during Retinal Surgery," in *Proc. IEEE 28th Annu. Northeast Bioengineering Conf.*, Philadelphia, USA, April 2002, pp. 171-172.
- [4] R.J. Elble and J.E. Randall, "Mechanistic Components of Normal Hand Tremor," *J. Electroencephalography and Clinical Neurophysiology*, vol. 44, no. 1, pp. 72-82, January 1978.
- [5] A. Uneri et al., "New Steady-Hand Eye Robot with Micro-Force Sensing for Vitreorectal Surgery," in *Intl. Conf. Biomed. Robotics & Biomechanics*, Tokyo, Japan, September 2010, pp. 814-819.
- [6] H. Das, H. Zak, J. Johnson, J. Crouch, and D. Frambach, "Evaluation of a Telerobotic System to Assist Surgeons in Microsurgery," *Comp. Aided Surg.*, vol. 4, no. 1, pp. 15-25, 1999.
- [7] W.T. Ang, P.K. Pradeep, and C.N. Riviere, "Active Tremor Compensation in Microsurgery," in *Proc. 26th Annu. Intl. Conf. IEEE Eng. Med. & Bio. Soc.*, Sept. 2004, vol. 1, pp. 2378-2741.
- [8] R.A. MacLachlan et al., "Micron: An Actively Stabilized Handheld Tool for Microsurgery," *IEEE Trans. Robotics*, vol. 28, no. 1, pp. 192-212, February 2012.
- [9] C. Song, P.L. Gehlbach, and J.U. Kang, "Active Tremor Cancellation by a "Smart" Handheld Vitreoretinal Microsurgical Tool using Swept Source Optical Coherence Tomography," *Optics Express*, vol. 20, no. 21, pp. 23414-23421, Sept. 2012.
- [10] M. Shahinpoor and K.J. Kim, "Ionic Polymer-metal Composites I: Fundamentals," *Smart Materials and Structures*, vol. 10, no. 4, pp. 819-833, August 2001.
- [11] W.T. Ang, P.K. Khosla, and C.N. Riviere, "Design of All-Accelerometer Inertial Measurement Unit for Tremor Sensing in Hand-held Microsurgical Instrument," in *Proc. IEEE Intl. Conf. Robotics and Automation*, vol. 2, Sept. 2003, pp. 1781-1786.
- [12] E.R. Bachmann, X. Yun, D. McKinnery, R.B. McGhee, and M.J. Zyda, "Design and Implementation of MARG Sensors for 3 DOF Orientation Measurement of Rigid Bodies," in *Proc. IEEE Intl. Conf. Robotics and Automation*, vol. 1, Sept. 2003, pp. 1171-1178.
- [13] W.T. Latt, U-X. Tan, K.C. Veluvolu, C.Y. Shee, and W.T. Ang, "Physiological Tremor Sensing using only Accelerometers for Real-time Compensation," in *Proc. 2008 IEEE Intl. Conf. on Robotics and Biomimetics*, February 2009, pp. 474-479.
- [14] U-X. Tan et al., "Estimating Displacement of Periodic Motion with Inertial Sensors," *IEEE J. Sensors*, vol. 8, no. 8, pp. 1385-1388, 2008.
- [15] A. Saxena and R.V. Patel, "Sensing Physiological Tremor in a Handheld Microsurgical Instrument," in *Proc. 2013 ASME Summer Bioeng. Conf.*, Sunriver, Oregon, USA, June 2013, paper no. 14185.
- [16] K. Jung, J. Nam, and H. Choi, "Investigations on actuation characteristics of IPMC artificial muscle actuator," *Sensors and Actuators A: Physical*, vol. 107, no. 2, pp. 183-192, October 2003.